

The Structure of Titanium Oxide in Titania (TiO₂) Photoactive Water-Splitting Catalysts by Raman Spectroscopy

Franklin D. Hardcastle, Hidetaka Ishihara, Rajesh Sharma, and Alexandru S. Biris, *Member, IEEE*

Abstract—Anodized TiO₂ films were modified in an effort to improve photoelectrochemical response using a low-pressure nitrogen plasma to provide N doping and carbon-dioxide annealing to provide carbon doping. Raman spectroscopy was used to identify amorphous and crystalline TiO₂ phases present in the films as well as the state of carbon and nitrogen species. The chemical composition of the film under different surface chemical modification treatments was correlated with photoelectrochemical (PEC) performance. The results show that oxygen-annealed Ti foil exhibits higher photocurrent densities compared unheated foil, and the increase is associated with rutile formation. Oxygen-annealed anodized TiO₂ films, associated with mixed crystalline anatase and rutile phases, also exhibit higher photocurrent densities. It is also shown that N₂ plasma treatment of the anodized films results in higher photocurrent densities and also promotes rutile formation. CO₂-annealing also increases the photocurrent density – the deposited carbon is shown to transform amorphous titania to anatase at higher temperatures with an increase in photocurrent density, but accelerates the transformation of anatase to rutile in the absence of amorphous titania.

Index Terms— Raman Spectroscopy, Titanium Oxide, Water-Splitting Catalyst

I. INTRODUCTION

For many years, bulk titania (TiO₂) has been investigated both as a photocatalyst for the decomposition of organic waste and as a potential water-splitting catalyst for generating hydrogen fuel from water. Recently, TiO₂ nanotubes and nanocrystalline titania have been investigated for the

photocatalytic splitting of water into hydrogen and oxygen using solar light. TiO₂ is a promising photoanode material for water splitting using solar radiation because of its favorable band structure, low cost, chemical stability, and photostability [1]. The most important requirement of a photocatalyst is its ability to generate electron-hole pairs by harvesting a significant portion of available solar radiation spectra. Unfortunately, the use of TiO₂ as a water-splitting catalyst is hindered by its inefficient use of solar energy in the visible region. The large bandgap of TiO₂ (3.0 eV for rutile and 3.2 eV for anatase) [2] only allows photoconversion of UV radiation, which comprises about 7% of the solar spectrum. Thus, bandgap reduction of TiO₂ is a key requirement for effective utilization of solar radiation.

Recent studies have shown a positive effect of plasma treatment on photocatalytic properties of TiO₂ particles [3], [4]. Nakamura *et al.* [3] studied the effect of plasma treatment on remediation of NO by TiO₂ particles and observed that hydrogen plasma treatment introduced the photocatalytic activity in the visible light region without affecting its activity in the UV region. Huang *et al.* [4] showed increased photocatalytic degradation of gaseous 2-propanol (IPA) with nitrogen plasma treated TiO₂. Changsheng *et al.* [5] showed improved photocatalytic activity of nitrogen plasma treated TiO₂ powders. Chiba *et al.* [6] showed that plasma treatment using Ar, H₂ and CH₄ shifted the absorption edge of TiO₂ thin film to the visible light region. A number of studies have focused on bandgap reduction of TiO₂ by doping with transition metal cations [7]-[9] and non-metallic anions including carbon [10]-[14]. In fact, Park *et al.* [13] reported carbon-doped TiO₂ (TiO_{2-x}C_x) nanotube arrays that showed much higher photocurrent densities and more efficient water splitting under visible-light illumination (>420 nm) than pure TiO₂ nanotube arrays, with a total photocurrent more than 20 times higher than that of a P-25 film under white-light illumination.

In this study, Nanotubular and nanocrystalline TiO₂ films were synthesized using electrochemical anodization of Ti foil. This was followed by chemical modification using a low-pressure nitrogen plasma and carbon doping by carbon-dioxide annealing in an effort to improve photoelectrochemical response. Raman spectroscopy is ideally suited for the study of metal oxides in general, but especially titanates since the Raman band positions are sensitive to changes in bond length

Manuscript received April 17, 2009. This work was supported in part by the United States Department of Energy Grant # GO86054 and Arkansas Science and Technology Authority.

F. D. Hardcastle is with the Department of Physical Sciences, Arkansas Tech University, Russellville, AR 72801 USA. He is also a research affiliate with the UALR Center of Nanotechnology, Little Rock, Arkansas 72204 (479-968-0619; e-mail: fhardcastle@atu.edu).

H. Ishihara is a graduate student with the University of Arkansas at Little Rock, UALR Center of Nanotechnology, Graduate Institute of Technology, 2801 S. University Ave., Little Rock, Arkansas 72204

R. Sharma is with the University of Arkansas at Little Rock, UALR Center of Nanotechnology, Graduate Institute of Technology, 2801 S. University Ave., Little Rock, Arkansas 72204

A. S. Biris is with the University of Arkansas at Little Rock, UALR Center of Nanotechnology, Graduate Institute of Technology, 2801 S. University Ave., Little Rock, Arkansas 72204.

and molecular geometry. For this reason, Raman spectroscopy was used to determine the amorphous and crystalline phases present in the titania films as well as to identify the state of carbon and nitrogen species present on the treated films.

II. EXPERIMENTAL PROCEDURE

A. Electrochemical Synthesis of TiO₂ Nanotubular Arrays

TiO₂ (titania) nanotubular and nanocrystalline structures, considered ideal for photoelectrolysis [15], were synthesized on the titanium metal foil support (99.9% pure, 0.5 mm thick) using a conventional anodization process (95 wt% ethylene glycol + 5 wt% NH₄F; 20V, 1 A, 1 h). A two-electrode configuration was used for anodization. A platinum electrode (thickness: 1 mm; area: 3.75 cm²) served as a cathode. The distance between the two electrodes was kept at 4.5 cm in all the experiments. Anodization was carried out at a constant potential of 20 V using a DC voltage supply (Agilent, E3640A). The anodization current was monitored continuously using a digital multimeter (METEX, MXD 4600 A). After an initial increase–decrease transient, the current reached a steady-state value. The anodized samples were washed with distilled water to remove the occluded ions from the anodized solutions and dried in an air-oven.

B. Plasma Surface Treatment

The TiO₂ films were plasma treated following the anodization and subsequent air-drying, but prior to thermal treatments. The plasma reactor consists of two parallel aluminum electrodes. The plasma was generated between the electrodes using a 13.56 MHz RF power supply (MCS Plasma Systems Model HF-3) with an impedance matching network. Samples were placed in a ceramic boat between the electrodes. The reactor consisted of a unique gas flow design where gas was dispersed into the chamber using a series of inlets from the top electrode. Nitrogen was used as processing gas with an operating pressure of 150 mTorr. The samples were routinely exposed to an argon “cleaning” plasma 5 min followed by the nitrogen plasma for 1 h.

C. Oxygen and Carbon Dioxide Annealing

The anodized and anodized/plasma-treated Ti samples were annealed in an oxygen atmosphere at 400–600°C for 6 h in a tube furnace to convert the amorphous titania to the crystalline anatase and/or rutile forms of TiO₂. The carbon dopant was introduced to the nanocrystalline TiO₂ by heating at 600°C under controlled CO₂ gas flow.

D. Photoelectrochemical (PEC) Characterization

Photocurrent densities were measured as a function of plasma treatment, oxygen annealing, and heating in carbon dioxide (to incorporate carbon). Current versus potential measurements were performed using a Perkin-Elmer Model 283 Potentiostat / Galvanostat (EG&G Instruments Corp.) and typical three-electrode electrochemical cell (Pt-wire counter electrode, saturated Ag/AgCl reference electrode). PEC

studies were carried out in a glass cell with separate compartments for the photoanode (nanotubular TiO₂ specimen) and the cathode (Pt wire). The compartments were connected by a fine porous glass frit. A reference electrode (Ag/AgCl) was placed closer to the anode using a salt-bridge (saturated KCl)-Luggin probe capillary. The cell was provided with a 60-mm diameter quartz window for light incidence. A 300-W solar simulator (Model: 69911, Newport-Oriel Instruments, Stratford, CT, USA) was used as a light source. The electrolyte used was 1 M KOH (pH ~ 14) aqueous solution. The electrolyte was prepared using reagent grade chemicals and double-distilled water. No aeration was carried out to purge out the dissolved gases in the electrolyte. A potentiostat interfaced with a computer and software (Model: PC3/CMS 100, Gamry Instruments Inc., Warminster, PA, USA) was employed to control the potential and record the photocurrent. The samples were anodically polarized from the open circuit potential until 0.5 V at a scan-rate of 5 mV s⁻¹ under illumination and the photocurrent was recorded.

E. Raman Spectroscopy

Raman spectra of all TiO₂ films were collected using a LabRam Micro-Raman Spectrometer (Horiba Jobin-Yvon HR800 UV) equipped with an optical microscope and 100x objective lens for a total magnification 1000x. An argon-ion laser (524.5 nm) or helium-neon (632.8 nm) was used for laser excitation of the Raman signal with appropriate holographic notch filters for eliminating the laser line after excitation. The laser power at the sample ranged from 1 to 3 mW, and the 1/e laser spot size was about 2 μm at the sample. The slit width of the spectrometer was typically set at 700 μm. An 1800 grooves/mm grating was used which resulted in a spectral resolution of about 1.5 cm⁻¹.

III. RESULTS

A. Photoelectrochemical (PEC) Characterization

Table I shows the photocurrents obtained from un-anodized Ti foil, anodized Ti foil, and Ti foil that was anodized and plasma-treated, respectively, all as a function of O₂-annealing temperature (25°C, or air-dried, up to 600°C for 6 h). The photocurrent density for the Ti foil samples that were not anodized increased from 20 μA cm⁻² for as-purchased Ti foil up to 277 μA cm⁻² for Ti foil O₂-annealed at 600°C.

Table I
Photocurrent Densities for TiO₂ Films (microamps per cm²)

O ₂ Annealing Temperature -->	25°C	500°C	600°C
Not Anodized	20	166	277
Anodized	20	379	
CO ₂ Annealed (600°C)		430	581
Anodized + Plasma	20	440	497
CO ₂ Annealed (600°C)		450	

For samples that were anodized (95 wt% ethylene glycol + 5 wt% NH_4F ; 20V, 1 A, 1 h), the photocurrent increased from 20 $\mu\text{A cm}^{-2}$ for the air-dried, room-temperature sample up to 379 $\mu\text{A cm}^{-2}$ for the sample O_2 -annealed at 500°C (data are not yet available for the sample treated at 600°C). When this sample was annealed in CO_2 at 600°C for 6 h, the photocurrent increased from 379 to 430 $\mu\text{A cm}^{-2}$. The highest photocurrent of 581 $\mu\text{A cm}^{-2}$ was measured for anodized samples O_2 -annealed for 6 h at 600°C, followed by CO_2 -annealing at 600°C for 6 h.

For plasma-treated samples (Ar plasma, 5 min; N_2 plasma, 150 mTorr, 1 h), the photocurrent increased from 20 $\mu\text{A cm}^{-2}$ for the air-dried, room-temperature sample up to 440 $\mu\text{A cm}^{-2}$ for the sample O_2 -annealed (500°C) and increased to 497 $\mu\text{A cm}^{-2}$ for O_2 -annealed (600°C). There was a slight decrease in photocurrent to 450 $\mu\text{A cm}^{-2}$ when O_2 -annealed (500°C) was CO_2 -annealed at 600°C (data are not yet available for the sample CO_2 -annealed at 600°C).

It was noted that the open circuit potentials (OCP) of the N_2 -plasma treated samples were more negative than those of untreated samples, decreasing from -0.85 to -0.97 V after plasma treatment. The OCP values at dark ranged from -0.3 to -0.4 V. This negative shift in OCP values after illumination indicates an increase in band bending after plasma treatment. Since the OCP values reflect the difference between the Fermi level of semiconductor and redox potential of the electrolyte, a more negative value of OCP is preferred.

B. Raman Spectroscopy

The Raman spectra for the un-anodized Ti foil as a function of O_2 -annealing temperature is presented in Fig. 1. The major band positions at 610, 446, and 242 cm^{-1} are consistent with the rutile phase of TiO_2 . These peaks are initially observed for the sample annealed at 400°C and become sharper and more intense as the annealing temperature is increased indicating increasing crystallinity of the rutile phase. The unheated Ti foil exhibits broad bands near 600 and 300 cm^{-1} characteristic of amorphous titania.

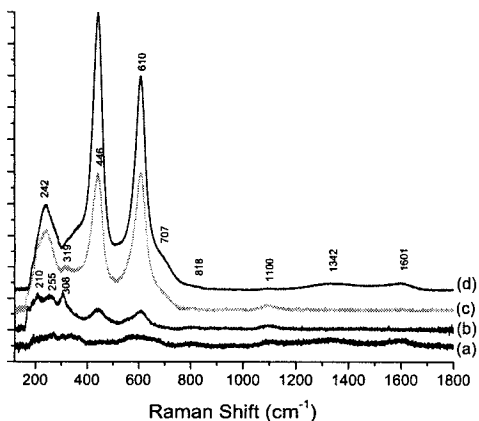


Fig. 1. Raman spectra of untreated Ti foil (a) as purchased, and O_2 -annealed at (b) 400°C, (c) 500°C, and (d) 600°C.

Carbon is present as indicated by the characteristic bands near 1342 and 1601 cm^{-1} , assigned to sp^3 - and sp^2 -hybridized carbon bonding, respectively. Carbonate, CO_3^{2-} , is present in all these samples as indicated by the characteristic band near 1100 cm^{-1} .

The Raman spectra for the Ti foil samples that were anodized (95 wt% ethylene glycol + 5 wt% NH_4F ; 20V, 1 A, 1 h) and annealed in oxygen are presented in Fig. 2 as a function of O_2 -annealing temperature. The sample dried at room temperature shows broad peaks near 600 and 467 cm^{-1} due to amorphous titania. The remaining peaks are decomposition products of the ethylene glycol anodization solution; it is further noted that none of these peaks match those of ethylene glycol. The peak near 1598 cm^{-1} is characteristic of sp^2 -hybridized (graphitic-type bonding) carbon. The peak at 1076 cm^{-1} is characteristic of a carbonate species, CO_3^{2-} . Annealing in oxygen at 400°C for 6 h results in the formation of anatase as the dominant phase as well as a small amount of rutile. Anatase exhibits Raman bands at 635, 514, 396, 197 cm^{-1} and a very intense lattice vibration at 144 cm^{-1} . As the oxygen annealing temperature is increased from 400 to 600°C, the relative amount of rutile increases, with major band positions at 612, 446, and 238 cm^{-1} . For the anodized sample O_2 -annealed at 600°C, both anatase and rutile are present, with rutile being the dominant phase. This qualitative assessment is based on the experimental observation that the relative Raman cross sections of the rutile peak at 446 cm^{-1} and the anatase peak at 396 cm^{-1} are approximately equivalent.

The Raman spectra for Ti foil samples that were anodized (95 wt% ethylene glycol + 5 wt% NH_4F ; 20V, 1 A, 1 h), plasma-treated with argon (5 min) and nitrogen (1 h), then annealed in oxygen are presented in Fig. 3 as a function of O_2 -annealing temperature. The sample dried at room temperature is almost identical to that of the anodized sample (see Fig. 2) showing bands at 600 and 467 cm^{-1} due to amorphous titania, decomposition of ethylene glycol, carbon, and carbonate. An important difference between the spectrum of the anodized dried sample (Fig. 2) and that of the anodized/plasma-treated

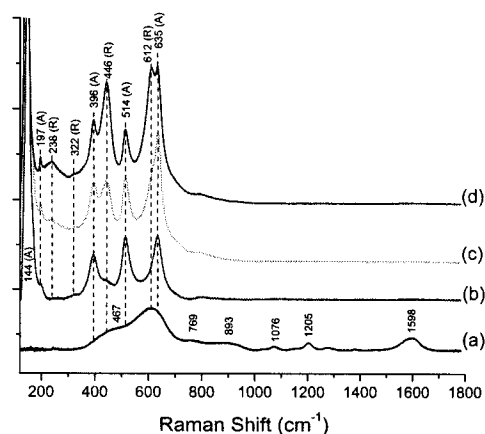


Fig. 2. Raman spectra of anodized Ti foil after (a) room-temperature drying, and O_2 -annealed at (b) 400°C, (c) 500°C, and (d) 600°C.

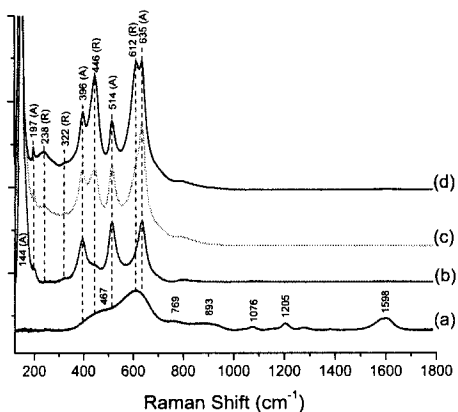


Fig. 3. Raman spectra of anodized Ti foil that was plasma-treated (He for 5 min, N₂ for 1 h) (a) room-temperature drying, and O₂-annealed at (b) 400°C, (c) 500°C, and (d) 600°C.

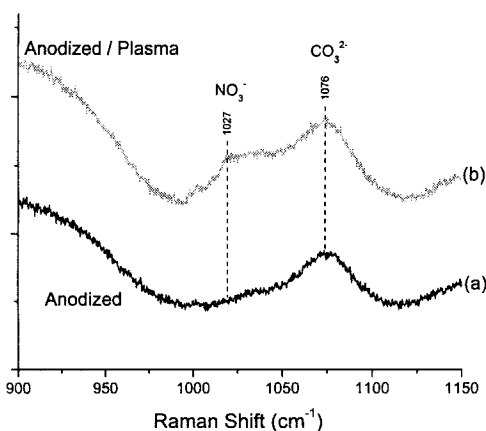


Fig. 4. Raman spectra of (a) anodized and (b) anodized / plasma-treated Ti foil samples, dried at room temperature, showing the presence of nitrate and carbonate.

dried sample (Fig. 3) is the 1027-cm⁻¹ band characteristic of nitrate species, NO₃⁻, presumably originating from the N₂ plasma. Fig. 4 compares this spectral region for the room-temperature dried samples.

Very similar to the anodized samples (Fig. 2), the plasma-treated sample annealed in oxygen at 400°C results in the formation of anatase (635, 514, 397, 197, 144 cm⁻¹) and a small amount of rutile (612, 446, 397, 237 cm⁻¹). For samples annealed at 500 and 600°C, both anatase and rutile are present, with rutile being the dominant phase. But there is noticeably more rutile compared to comparable samples that were simply anodized and not plasma-treated (Fig. 2).

The Raman spectra for Ti foil samples that were anodized and annealed in oxygen at 500°C and 600°C are presented in Fig. 5(a) and 5(b), respectively. These spectra are compared with those of the same samples after being annealed in CO₂ for 6 h, presented in Fig. 5(c) and 5(d), respectively. Carbon deposition on the films was verified by monitoring Raman bands near 1600 cm⁻¹ (sp²-hybridized; graphitic-like bonding) and 1337 cm⁻¹ (sp³-hybridized; diamond-like bonding), the

presence of both peaks are characteristic of a 'carbon black' material. The anodized O₂-annealed (500°C) film, Fig. 5(a), shows equivalent amounts of rutile and anatase. As the O₂-annealing temperature is increased to 600°C, the relative amount of rutile increases, noted by the increase in the relative intensity of the bands at 610 and 443 cm⁻¹, Fig. 5(b). If, instead of O₂-annealing the 500°C sample at 600°C, this sample were CO₂-annealed at 600°C, significantly more anatase would result as shown by Fig. 5(c). Since the transformation of rutile to anatase is not thermodynamically favored, it is likely that the amorphous titania present in the 500°C sample transformed to anatase in the presence of the carbon deposited by the CO₂ annealing.

The O₂-annealed (600°C) anodized film, Fig. 5(b), contains slightly more rutile than anatase. After CO₂-annealing this sample for 6 h, all of the remaining anatase transformed to rutile as shown in Fig. 5(d).

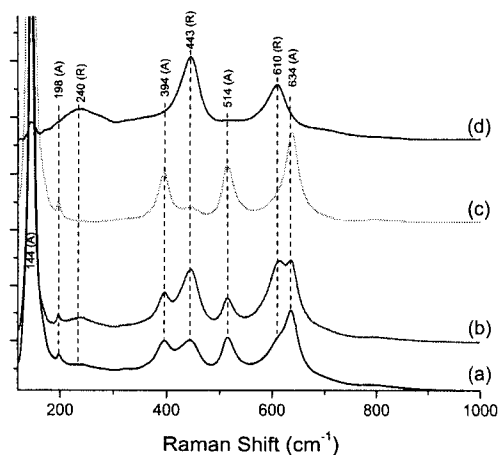


Fig. 5. Raman spectra of anodized films O₂-annealed at (a) 500°C and (b) 600°C. Raman spectra of anodized films (c) O₂-annealed at 500°C, then CO₂-annealed at 600°C, and (d) O₂-annealed at 600°C, then CO₂-annealed at 600°C.

The Raman spectra for Ti foil samples that were anodized, plasma-treated, and annealed in oxygen at 500°C and 600°C are presented in Fig. 6(a) and 6(b), respectively. These spectra are compared with those of the same samples after being annealed in CO₂ for 6 h, presented as Fig. 6(c) and 6(d), respectively. The O₂-annealed (500°C) film, Fig. 6(a), shows approximately equivalent amounts of rutile and anatase, and the relative amount of rutile increases for the O₂-annealing (600°C) film, Fig. 6(b). If, instead of O₂-annealing the 500°C sample at 600°C, the sample were CO₂-annealed at 600°C, significantly more anatase results as shown by Fig. 6(c). Since the transformation of rutile to anatase is not thermodynamically favorable, it is likely that the amorphous titania present in the O₂-annealed (500°C) film transformed to anatase in the presence of the carbon deposited by CO₂ annealing.

The anodized O₂-annealed (600°C) film, Fig. 6(b), shows a higher relative amount of rutile versus anatase. After CO₂-annealing this sample for 6 h, the anatase/rutile composition

remains constant, as shown in Fig. 6(d), although the crystallinity is increased as evidenced by the sharper bands.

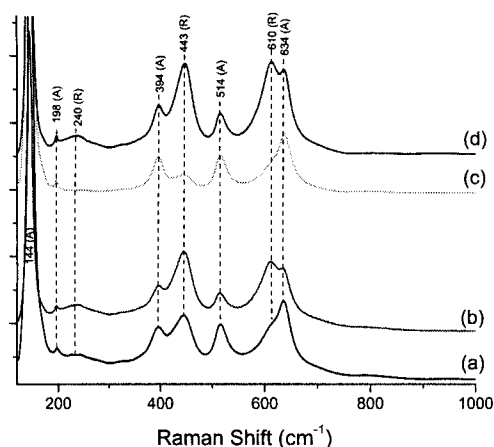


Fig. 6. Raman spectra of anodized and plasma-treated films O₂-annealed at (a) 500°C and (b) 600°C. Raman spectra of anodized and plasma-treated films (c) O₂-annealed at 500°C, then CO₂-annealed at 600°C, and (d) O₂-annealed at 600°C, then CO₂-annealed at 600°C.

IV. DISCUSSION

A. Untreated Ti Foil Samples

The TiO₂ phases and other chemical species identified by Raman spectroscopy are presented in Table II. The Raman results show that O₂-annealed Ti foil samples exhibit higher photocurrent densities compared with samples that were not annealed in oxygen. For untreated, unheated Ti foil, amorphous titania, carbon (similar to carbon black), and carbonate are present as shown in Fig. 1 and summarized in

Table II
Phases Present in TiO₂ Films

O ₂ Annealing Temp.	25°C	400°C	500°C	600°C
Not Anodized	Am C / CO ₃ ²⁻	Am>R CO ₃ ²⁻	R>Am CO ₃ ²⁻	R C / CO ₃ ²⁻
Anodized	Am dEG/CO ₃ ²⁻	Am/A>>R	A/R	R>A
CO ₂ Annealed			A>>R	R
Anodized + Plasma	Am dEG/CO ₃ ²⁻ NO ₃ ⁻	Am/A>>R	A/R	A/R
CO ₂ Annealed			A>>R	R>A

Am: amorphous titania; A: anatase; R: rutile; C: carbon; CO₃²⁻: carbonate; NO₃⁻: nitrate; dEG: decomposed ethylene glycol

Table II. Annealing in oxygen from 400 to 600°C results in a gradual increase in rutile at the expense of the amorphous titania. At 600°C only rutile phase is present (with a small

amount of carbon and carbonate). Table I shows the photocurrent density increases from 20 μA cm⁻² for the air-dried, room-temperature sample up to 277 μA cm⁻² for the O₂-annealed (600°C) film where well-ordered, crystalline rutile is present. These results suggest that rutile exhibits a higher photocurrent density than amorphous titania.

B. Anodized TiO₂ Films

The PEC results show that anodized films that were O₂-annealed exhibit higher photocurrent densities than those that were not anodized, or samples that were only anodized and not O₂-annealed, consistent with recent work [16]. Fig. 2 and Table II show that the amorphous titania, present at room temperature, is converted mostly to anatase at 400°C, but the relative concentration of rutile increases at higher temperatures. At 600°C, both anatase and rutile are present. Table I shows the photocurrent density increases from 20 μA cm⁻² for the air-dried, room-temperature sample up to 379 μA cm⁻² for the O₂-annealed (600°C) film where well-ordered, crystalline rutile and anatase are present. These results suggest that a mixture of crystalline anatase and rutile exhibits a higher photocurrent density than amorphous titania. It has been suggested that upon annealing, the increased crystallinity results in enhanced charge transfer and photocatalytic activity [17].

C. Anodized / Plasma-Treated Films

Plasma treatment of TiO₂ films potentially offers many advantages for increasing photocatalytic reactivity. The ultraviolet radiation in a glow-discharge plasma is highly energetic, capable of breaking covalent chemical bonds [18], and contains reactive ions, free electrons, and radicals assist to remove contaminants from the surface. Plasma treatment has also been shown to increase the surface area of TiO₂ nanostructures [19], resulting in higher electrode/electrolyte interfacial contact area further enhancing the charge transfer.

The first step in our plasma treatment is to expose the films to an argon plasma for 5 min. Jun *et al.* [20] showed that argon plasma treatment acts both to clean the surface and to convert Ti⁴⁺ to Ti³⁺ and O²⁻ to O⁻. This surface cleaning due to plasma treatment is an important factor that contributed towards enhanced PEC properties for plasma treated samples. Sharma *et al* [16] showed that the plasma treatment reduced the oxygen on the surface and generated oxygen vacancies as evidenced by a decrease in the O/Ti ratio as measured by X-ray photoelectron spectroscopy (XPS). The conversion of Ti⁴⁺ sites to Ti³⁺ sites is believed to be facilitated by the creation of oxygen vacancies [21]. These defects were found to enhance the affinity of the surface to chemisorbed water making the surface more hydrophilic.

In this study, it is shown that anodized TiO₂ films that were plasma-treated and O₂-annealed exhibit higher photocurrent densities as compared to anodized films that were not plasma treated. Fig. 3 and Table II show an amorphous-to-crystalline transformation for the plasma-treated films that is almost identical to that of the anodized films (Fig. 2), except for the

presence of higher relative amounts of rutile. It is generally observed that the N₂ plasma treatment (which results in significant nitrogen doping of the film) enhances the formation of rutile over anatase at higher O₂-annealing temperatures of 500 and 600°C.

Table I shows the photocurrent density increases from 20 μA cm⁻² for the air-dried anodized/plasma-treated film up to 497 μA cm⁻² for the same film O₂-annealed (600°C) where well-ordered, crystalline rutile and anatase are present. Once again, these results suggest that a mixture of crystalline anatase and rutile exhibits a higher photocurrent density than amorphous titania. There is also an increase in photocurrent density (from 379 to 440 μA cm⁻²) associated with the N₂ plasma treatment for the anodized O₂-annealed (500°C) sample showing that plasma treatment resulted in positive effects on the photoactivity of TiO₂ films that were both anodized and O₂-annealed, consistent with the recent work of Sharma *et al.* [16].

Another important consequence of nitrogen plasma treatment is the change in surface chemical structure resulting in surface doping of TiO₂ by N atoms. Presumably, N atoms replace some oxygen atoms and/or oxygen vacancies. Recent XPS results show an increase in nitrogen concentration on the surface of anodized N₂-plasma treated TiO₂ films, increasing from 0.24 to 1.21 atom % after plasma treatment [16] as well as an XPS binding energy consistent with substitutional doping of N. The present work shows a significant increase in the amount of nitrogen, present as nitrate (Raman band at 1027 cm⁻¹), for the dried anodized/plasma-treated films. It has been suggested that N atoms hybridize with the O 2p valence band resulting in delocalization of the nitrogen valence electrons and an upward shift of the valence band maximum [22]. The creation of oxygen vacancies coupled with the substitutional N doping reduce the bandgap of TiO₂ on the surface. In perspective, however, the increase in photocurrent density after plasma treatment could be ascribed to a combination of several factors including removal of surface contaminants, change in surface physical structure, and modification of surface chemical structure causing changes in surface energetics as well as overall changes in bulk chemistry.

D. Anodized and Anodized / Plasma-Treated Films Annealed in Carbon Dioxide

The presence of carbon (from CO₂ deposition) is shown to transform amorphous titania to anatase (500°C, O₂-annealed samples), and to accelerate the transformation of anatase to rutile in the absence of amorphous titania (600°C, O₂-annealed samples). For anodized and anodized/plasma-treated TiO₂ films, O₂-annealing at 400°C transforms the amorphous titania almost exclusively to anatase, at 500°C to a mixture that is more anatase than rutile, and at 600°C to mixture having comparable amounts of anatase and rutile. The phases present for the anodized plasma-treated samples are very similar, but show slightly more rutile.

For the anodized O₂-annealed (500°C) sample (more anatase than rutile; 379 μA cm⁻²), annealing in O₂ at 600°C results in a

comparable anatase/rutile mixture whereas annealing in CO₂ instead of O₂ at 600°C results in almost all anatase (430 μA cm⁻²). Presumably the carbon-doping affects the transformation of amorphous titania (present in the O₂-annealed (500°C) sample) and is either enhancing the anatase transformation or interfering with the thermodynamically preferred transformation to rutile.

For the O₂-annealed (600°C) samples, the anatase/rutile mixture is unaffected by repeated O₂-annealing at 600°C. At this temperature, a significant amount of amorphous titania is unlikely and all the TiO₂ should be crystalline as rutile or anatase. Annealing this sample in CO₂ at 600°C results in a complete transformation of all the TiO₂ to rutile (581 μA cm⁻²). It is inferred that when there is no amorphous titania present, carbon acts to accelerate the anatase-to-rutile transformation.

It is generally observed that plasma-treatment (N doping) enhances rutile formation. For plasma-treated samples that are CO₂-annealed, there is competition between the effects of the nitrogen plasma (promoting rutile formation) and the effects of carbon (anatase formation for samples O₂-annealed at 500°C; rutile formation for samples O₂-annealed at 600°C). In particular, the highest photocurrent density measured in the present study is 581 μA cm⁻² for the anodized O₂-annealed (600°C) / CO₂-annealed (600°C) film which is composed of crystalline rutile. The photocurrent has not yet been measured for the plasma-treated analogue which is composed of comparable amounts of anatase and rutile.

V. CONCLUSION

In this work, anodized TiO₂ films were modified in an effort to improve photoelectrochemical response using a low-pressure nitrogen plasma to provide N doping and carbon-dioxide annealing to provide carbon doping. Raman spectroscopy served as an effective method of identifying amorphous and crystalline TiO₂ phases present in the films as well as the state of carbon and nitrogen species. The chemical composition of the film under different surface chemical modification treatments was correlated with photoelectrochemical (PEC) performance.

The present results show that Ti foil samples that were O₂-annealed exhibit higher photocurrent densities compared with samples that were not annealed in oxygen. The significant increase in photocurrent (14 times baseline) is associated with the rutile phase of TiO₂.

Samples anodized and O₂-annealed exhibit higher photocurrent densities as compared to samples that were not anodized, or samples that were only anodized and not O₂-annealed. Anodization results in the formation of a thick film of amorphous titania, which is converted to mostly anatase at 400°C, but rutile forms at higher temperatures. The photocurrent increases significantly (19 times baseline) at 500°C where the crystallinity of anatase and rutile increases.

It is also shown that N₂ plasma treatment of the surface

incorporates nitrogen into the anodized TiO₂ film as a nitrate species, promotes slightly more rutile formation, and results in higher photocurrent densities (25 times baseline for O₂-annealed at 600°C; 16% higher versus comparable sample not treated with plasma).

Carbon deposition by CO₂-annealing is shown to transform amorphous titania to anatase at (500°C, O₂-annealed samples) with an increase in photocurrent density (21 times baseline; 13% higher than anodized-annealed sample), and to accelerate the transformation of anatase to rutile in the absence of amorphous titania (600°C, O₂-annealed samples) (29 times baseline; all rutile).

For plasma-treated samples that are CO₂-annealed, there is competition between the effects of the nitrogen plasma (promoting rutile formation) and the effects of carbon (anatase formation for samples O₂-annealed at 500°C; rutile formation for samples O₂-annealed at 600°C).

ACKNOWLEDGMENT

The authors gratefully acknowledge financial support from the United States Department of Energy Grant # GO86054 and Arkansas Science and Technology Authority.

REFERENCES

- [1] C. Burda, Y. Lou, X. Chen, A. C. S. Semia, J. Stout, and J. L. Gole *Nano Lett.* **3**, 1049-1051 (2003).
- [2] A. Bendavid, P. J. Martin, A. Jamting, and H. Takikawa, *Solid Films* **356** 6-11 1999.
- [3] I. Nakamura, N. Negishi, S. Kutsuna, T. Ihara, S. Sugihara, and K. Takeuchi *J. Mol. Catal. A* **161** 205 2000.
- [4] C. M. Huang, L. C. Chen, K. W. Cheng, and G. T. Pan *J. Mol. Catal. A* **261** 218 2007.
- [5] L. Changsheng, M. A. Zhibin, J. Li, and W. Weihong *Plasma Sci. Technol.* **8** 311 2006.
- [6] Y. Chiba, K. Kashiwagi, and H. Kokai *Vacuum* **74** 643 2004.
- [7] W. Choi, A. Termin, and M. R. Hoffmann *J. Phys. Chem.* **98** 13669 1994.
- [8] A. K. Ghosh and H. P. Maruska *J. Electrochem. Soc.* **124** 1516 1977.
- [9] H. Yamashita, M. Honda, M. Harada, Y. Ichihashi, M. Anpo, T. Hirao, N. Itoh, and N. Iwamoto *J. Phys. Chem. B* **102** 10707 1998.
- [10] S. Sato *Chem. Phys. Lett.* **123** 126 1986.
- [11] R. Asahi, T. Morikawa, T. Ohwaki, K. Aoki, and Y. Taga *Science* **293** 269 2001.
- [12] S. U. M. Khan, M. Al-Shahry, and W. B. Ingler, Jr *Science* **297** 2243-4 2002.
- [13] J. H. Park, S. Kim, and A. J. Bard *Nano Lett.* **6** 24 2006.
- [14] T. Umebayashi, T. Yamaki, and H. Itoh *Appl. Phys. Lett.* **81** 454 2002.
- [15] C. A. Grimes *J. Mater. Chem.* **17** 1451 2007.
- [16] R. Sharma, P. P. Das, M. Misra, V. Mahajan, J. P. Bock, S. Trigwell, A. S. Biris, and M. K. Mazumder *Nanotechnology* **20** 075704 2009.
- [17] J. F. Porter, Y. Li, and C. K. Chan *J. Mater. Sci.* **34** 1523 1999.
- [18] D. T. Clark and A. Dilks *J. Polym. Sci. Polym. Chem. Edn* **17** 957 1979.
- [19] R. Sharma, J. J. Diaz, V. Saini, A. S. Biris, and M. K. Mazumder *Presented at the Electrostatic Society of America Annual Meeting (West Lafayette, IN: Purdue University) 2007.*
- [20] J. Jun, J. H. Shin, and M. Dhayal *Appl. Surf. Sci.* **252** 3871 2006.
- [21] R. Wang, K. Hashimoto, A. Fujishima, M. Chikuni, E. Kojima, A. Kitamura, M. Shimohigoshi, and T. Watanabe *Adv. Mater.* **10** 135 1998.
- [22] R. Asahi, T. Morikawa, T. Ohwaki, K. Aoki, and Y. Taga *Science* **293** 269 2001.